DTU Library

Closed-Loop Two-Stage Stochastic Optimization of Offshore Wind Farm Collection System

Pérez-Rúa, Juan-Andrés; Lumbreras, Sara; Ramos, Andres; Cutululis, Nicolaos Antonio

Published in:
Journal of Physics: Conference Series

Link to article, DOI:
10.1088/1742-6596/1618/4/042031

Publication date:
2020

Document Version
Publisher's PDF, also known as Version of record

Journal of Physics: Conference Series

PAPER • **OPEN ACCESS**

Closed-Loop Two-Stage Stochastic Optimization of Offshore Wind Farm Collection System

To cite this article: Juan-Andrés Pérez-Rúa *et al* 2020 *J. Phys.: Conf. Ser.* **1618** 042031

Closed-Loop Two-Stage Stochastic Optimization of Offshore Wind Farm Collection System

Juan-Andrés Pérez-Rúa[1], Sara Lumbreras[2], Andrés Ramos[2] and Nicolaos A. Cutululis[1]

[1]DTU Wind Energy, Technical University of Denmark, Frederiksborgvej 399, 4000 Roskilde, Denmark.
[2]Institute for Research in Technology, Comillas Pontifical University, Calle de Alberto Aguilera 23, 28015 Madrid, Spain.

E-mail: juru@dtu.dk

Abstract. A two-stage stochastic optimization model for the design of the closed-loop cable layout of an Offshore Wind Farm (OWF) is presented. The model consists on a Mixed Integer Linear Program (MILP) with scenario numeration incorporation to account for both wind power and cable failure stochasticity. The objective function supports simultaneous optimization of: (i) Initial investment (network topology and cable sizing), (ii) Total electrical power losses costs, and (iii) Reliability costs due to energy curtailment from cables failures. The mathematical optimization program is embedded in an iterative framework called PCI (Progressive Contingency Incorporation), in order to simplify the full problem while still including its global optimum. The applicability of the method is demonstrated by application to a real-world instance. The results show the functionality of the model in quantifying the economic profitability when applying stochastic optimization compared to a deterministic approach, given certain values of cables failure parameters.

1. Introduction

Offshore Wind Farms (OWFs) are shaping up as one of the main drivers towards the transition to carbon-neutral power systems. Ambitious targets set by the European Commission see offshore wind power reaching 450 GW by 2050 [1]. Offshore electrical systems have a sizeable weight in the capital investments, reaching 15% of the total initial costs [2], with the power cables being a backbone component for the Balance of Plants (BoP) value. Furthermore, power cables can be single points of failure, leading to strongly undesired contingencies [3]. Shallow waters, buried depth, seabed terrain movements [4], and electro-thermal stress, are differential factors in the context of OWFs, resulting in higher failure rates of submarine cables compared to offshore industries, such as oil and gas [5] [6].

OWF export cables are generally built with redundancy, as the high voltage levels and long distances increase the failure probability [4]. Likewise, cables for collection systems may also be arranged to provide greater levels of reliability, typically resulting in a closed-loop topology. However, tailor-made models to design collection system with a closed-loop structure, using global optimization, integrated with analytical methods for reliability assessment, are not readily available in the scientific literature. Radial topology, i.e., without electrical redundancy (trees according to graph theory [7]) has been the most common subject of study in literature in this context, and currently represents the most frequent choice by OWF developers. However, with the increase in the OWFs' capacities and the trend of moving towards subsidy-free operating regimes, quantification of economic suitability for closed-loop or radial topologies is becoming essential.

Radial topology for OWF collection systems falls into a standard class of computational problems, being classified in computational complexity as NP-Hard [8]. Thus, scalability is the main challenge, as state-of-the-art OWFs are in the order of hundred of Wind Turbines (WTs). Mathematical models are proposed and solved through global optimization solvers in [9], [8], [10], [11], and [12]. Nevertheless, a deterministic approach is followed assuming no cable failure over the project lifetime.

Contrarily, studies adopting stochastic techniques are available in [13], [14], and [15]. A Mixed Integer Quadratic Program is presented in [13], which aims to analyze the suitability of having redundancy for system components subject to failure, by solving the full stochastic optimization program including all possible contingencies. Model reduction implementing a Mixed Integer Linear Program along with Progressive Contingency Incorporation (PCI), and decomposition strategies is performed in [14] and [15], proving the ability to reduce computational needs while solving to optimality small-scale OWFs (up to 30 WTs).

These papers provide relevant advances in stochastic optimization supporting several wind power and cable failure scenarios. Nonetheless, the inclusion of practical engineering constraints such as non-crossing of cables, closed-loop topology, and electrical losses in the objective function are not included in these papers. This gap is covered in this manuscript, where a MILP optimization program based computational model is presented, supporting decision makers during the design stage of OWFs. An algorithmic framework is developed targeting further computational simplification, supporting an objective function combining simultaneously initial investment, total electrical power losses, and energy curtailment due to cables failures. A recourse problem (minimizing the expected cost for energy curtailment) is solved, assessing the benefits of stochastic optimization compared to the deterministic counterpart.

The paper is structured as follows: In Section 2 the optimization model is explained in detail; followed by Section 2.2.2, where the algorithmic framework is explained. Finally, a case study is performed in Section 2.2.2. The work is finalized with the conclusions in Section 5.

2. Optimization model

2.1. Graph and model representation

The aim of the optimization is to design a closed-loop cable layout of the collection system for an OWF, i.e., to interconnect through power cables the n_{w} WTs to the Offshore Substation (OSS), while providing a redundant power evacuation route.

Let $\boldsymbol{N}_{\mathrm{w}} = \{2, \cdots, 1+n_{\mathrm{w}}\}$. Similarly, let the points set be $\boldsymbol{N} = \{1\} \cup \boldsymbol{N}_{\mathrm{w}}$, where the element $i \in \boldsymbol{N}$, such as $i = 1$ is the OSS.

The Euclidean distance between the positions of the points i and j, is denoted by d_{ij}. These inputs are collected in a weighted undirected graph $G(\boldsymbol{N}, \boldsymbol{E}, \boldsymbol{D})$, where $\boldsymbol{N}$ is the vertex set, $\boldsymbol{E}$ the set of available edges arranged as a pair-set, and $\boldsymbol{D}$ the set of associated euclidean distances for each element $[ij] \in \boldsymbol{E}$, where $i \in \boldsymbol{N} \wedge j \in \boldsymbol{N}$.

In general, $G(\boldsymbol{N}, \boldsymbol{E}, \boldsymbol{D})$ is a complete undirected graph. It may be bounded by defining uniquely those edges connecting the $\upsilon < n_{\mathrm{w}}$ closest WTs to each WT, and by the $\sigma < n_{\mathrm{w}}$ edges directly reaching the OSS from the WTs.

Likewise, let $\boldsymbol{T}$ be a predefined list of available cable types, and $\boldsymbol{U}$ be the set of cable capacities sorted in non-decreasing order as in $\boldsymbol{T}$, being measured in Amperes (A), such that u_t is the capacity of cable $t \in \boldsymbol{T}$. Furthermore, each cable type $t \in \boldsymbol{T}$ has a cost per unit of length, c_t (including capital and installation costs), in such a way that $\boldsymbol{U}$ and $\boldsymbol{T}$ are both comonotonic. The

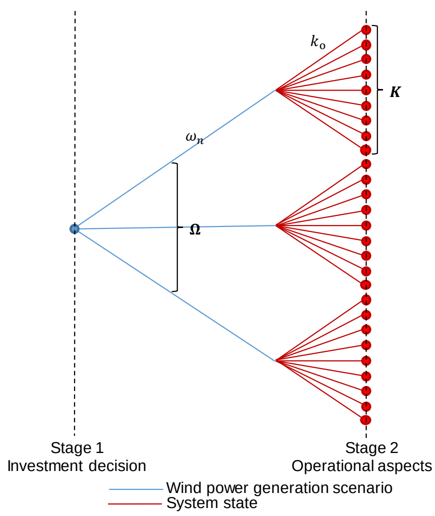

Figure 1. Scenario tree, Υ

set of cost per meter is defined as $\boldsymbol{C}$.

The problem is formulated as a stochastic optimization program with two stages: investment (construction) and operation. A graphical representation of the two stages is presented in Figure 1. Uncertainty is represented by a scenario tree (Υ), expressing simultaneously how the stochasticity is developing over time (at the moment of the investment decision, uncertainties of the random parameters are present), the different states of the random parameters (the instances of the random process multiply in function of the generation scenarios and installed cables), and the definition of the non-anticipative decisions in the present (in real-time operation the investment decision can not be changed).

The set of wind power generation scenarios is $\boldsymbol{\Omega}$ (blue lines in Figure 1), representing power states for wind speed regimes (inspired by the WT power curve and site capacity factor), while the representative system states are $\boldsymbol{K}$ (red lines in Figure Figure 1). The nominal generation scenario is ω_{n}, and the base system state (k_{o}) represents the case of no failures. The base case is therefore represented by the scenario $\{\omega_{\mathrm{n}}, k_{\mathrm{o}}\}$. A wind power generation scenario ω has associated a duration time τ^{ω} (in hours), and power magnitude ζ^{ω} (in per unit, p.u.), and each system state k, a system probability ψ^{k}. The cost of energy in €/Ah is denoted by c_{e}.

The system probability ψ^{k} is calculated using a discrete Markov model to define the cables' complementary states: available, and unavailable. Through this, it is possible to calculate ψ^{k} given the failure statistical parameters Mean Time Between Failures (MTBF) and Mean Time To Repair (MTTR) [16]. In the same way, given the low failure rates of these components a N-1 criterion must be considered in each system state [17]; this means that elements remaining in operation in a contingency are capable of accommodating the new operational situation, and it is very unlikely that other element would fail simultaneously.

The first stage variables are the binary variables $x_{ij,t}$, and y_{ij}; where $x_{ij,t}$ is equal to one if active edge $[ij]$ ($y_{ij} = 1$) uses cable type $t \in \boldsymbol{T}$. The second stage variables are the continuous variables $I_{ij}^{\omega,k}$, $\theta_{i}^{\omega,k}$, and $\delta_{j}^{\omega,k}$. The electrical current in edge $[ij]$ in wind power generation scenario $\omega \in \boldsymbol{\Omega}$, and system state $k \in \boldsymbol{K}$ is represented by $I_{ij}^{\omega,k}$, while the voltage phase at each WT busbar is $\theta_{i}^{\omega,k}$. The curtailed current at wind turbine j in wind power generation scenario $\omega \in \boldsymbol{\Omega}$, and system state $k \in \boldsymbol{K}$ is $\delta_{j}^{\omega,k}$. Note that $\delta_{j}^{\omega,k}$ is bounded by the current generated at j in the same scenario, I_{j}^{ω}, with $I_{j}^{\omega} = \frac{P_n \cdot \zeta^{\omega} \cdot 1000}{\sqrt{3} \cdot V_n}$, where P_n is the nominal power of an individual WT, and V_n the line-to-line nominal voltage of the system.

2.2. *Cost coefficients and objective function*

2.2.1. Neglecting total electrical power losses The objective function in this section consists of a simultaneous valuation of the total initial investment plus reliability. The investment is intuitively computed as the sum of cables costs installed in each edge $[ij]$; on the other hand, reliability is quantified through the estimation of the economic losses due to cables failures, as the result of undispatched current from each WT. In this way, the objective function is formalized as:

$$\min \overbrace{\sum_{[ij] \in \boldsymbol{E}} \sum_{t \in \boldsymbol{T}} c_t \cdot d_{ij} \cdot x_{ij,t}}^{\text{Investment}} + \overbrace{c_{\mathrm{e}} \cdot \sum_{i \in \boldsymbol{N}_{\mathrm{w}}} \sum_{\omega \in \boldsymbol{\Omega}} \sum_{k \in \boldsymbol{K}} \tau^{\omega} \cdot \psi^{k} \cdot \delta_{i}^{\omega,k}}^{\text{Operation/Reliability}} \tag{1}$$

The sum of system states probabilities must be equal to one, $\sum_{k \in \boldsymbol{K}} \psi^{k} = 1$, given the mutually exclusive nature of the considered events (at most one cable is subject to failure, N-1 criterion).

A system state k represents the failure of a single cable in an active edge $e \in \boldsymbol{E}$, therefore the system probability for the state ψ^{k} is considered equal to this failure probability. This implies that the availability probability of the other installed cables is considered to be equal to one in this scenario [13], representing a conservative approach as the value of the parameter ψ^{k} is slightly overestimated (the system probability is the multiplication of each installed cable state probability).

2.2.2. Considering total electrical power losses Total electrical power losses are non-linear in function of the current, cable type, and total length [7]. The designer must try to find a proper balance between modelling fidelity and optimization program complexity.

To include electrical losses in the objective function, a pre-processing strategy is proposed. This implies calculating the quadratic total electrical power losses in advance, and including the associated costs in the objective function.

The set of cable capacities in terms of number of maximum number of WTs is defined in the following expression

$$f_t = \left\lfloor \frac{\sqrt{3} \cdot V_n \cdot u_t}{P_n \cdot 1000} \right\rfloor \quad \forall t \in \boldsymbol{T} \tag{2}$$

Let the new cable type set be

$$\boldsymbol{T'} = \left\{ \underbrace{1, 2, \cdots, f_1}_{t_1}, \underbrace{f_1 + 1, \cdots, f_2}_{t_2}, f_2 + 1, \cdots, \underbrace{f_{|\boldsymbol{T}|-1} + 1, \cdots, f_{|\boldsymbol{T}|}}_{t_{|\boldsymbol{T}|}} \right\} \tag{3}$$

This implies that $\boldsymbol{T'}$ is the discretized form of the maximum capacity $U = \max \boldsymbol{U}$. Note that this is translated into the creation of additional variables $x_{ij,t'} : t' \in \boldsymbol{T'}$. Likewise, if the *floor function* in (2) is replaced by a *decimal round down function*, and $\boldsymbol{T'}$ is also discretized using the same decimal steps, then the number of variables will increase accordingly, to the benefit of gaining in accuracy for the cable capacities.

The non-dominated cable sub-types from $\boldsymbol{T}$ are contained in $\boldsymbol{T'}$; this means that each cable sub-type $t' \in \boldsymbol{T'}$ is related to a cable type $t \in \boldsymbol{T}$, inheriting physical properties such as cost per meter (c_t), electrical resistance per meter (R_t), and electrical reactance per meter (X_t); see (3) where this relation is presented graphically. Acknowledging that the investment cost of a cable t exceeds the electrical power losses costs, then the selected cable sub-type to connect n WTs will always be the cheapest (smallest) cable with sufficient capacity, rather than a bigger one with lower electrical power losses as the electrical resistance decreases with size.

As a consequence of the aforementioned, let a new cable capacities set be:

$$\boldsymbol{U'} = \left\{1, 2, \cdots, f_1, f_1 + 1, \cdots, f_2, f_2 + 1, \cdots, f_{|\boldsymbol{T}|-1} + 1, \cdots, f_{|\boldsymbol{T}|}\right\} \cdot \frac{P_n \cdot 1000}{\sqrt{3} \cdot V_n} \tag{4}$$

Let the functions $f(t')$, $g(t')$, and $h(t')$ calculate the cost, electrical resistance, and electrical reactance per meter for cable sub-type t', respectively, which are inherited from a cable type t. Whereby, the objective function for simultaneous optimization of investment, electrical losses, and reliability is:

$$\min \overbrace{\sum_{[ij] \in \boldsymbol{E}} \sum_{t' \in \boldsymbol{T'}} \left(f(t') + \underbrace{3 \cdot 1.5 \cdot g(t') \cdot \left(\frac{c_\text{e}}{\sqrt{3} \cdot V_n \cdot 1000} \right) \cdot \sum_{\omega \in \boldsymbol{\Omega}} \left(u'_{t'} \cdot \zeta^\omega \right)^2 \cdot \tau^\omega}_{=h(t').\ \text{Pre-processing for total electrical power losses}} \right) \cdot d_{ij} \cdot x_{ij,t}}^{\text{Investment plus total electrical power losses}} + \tag{5}$$

$$\overbrace{c_\text{e} \cdot \sum_{i \in \boldsymbol{N}_\text{w}} \sum_{\omega \in \boldsymbol{\Omega}} \sum_{k \in \boldsymbol{K}} \tau^\omega \cdot \psi^k \cdot \delta_i^{\omega,k}}^{\text{Operation/Reliability}}$$

The factor $(3 \cdot 1.5)$ in (5) accounts for the joule, screen and armouring losses for the three-phase system. The whole term for total electrical power losses ($h(t')$) is calculated for each $t' \in \boldsymbol{T'}$, before launching the MILP program into the external solver. Therefore, the objective function is a linear weighting of the desired targets: investment, electrical losses, and reliability.

As discussed previously, one of the tasks of the designer is to balance out modelling fidelity and optimization program complexity. The objective function in (5) is a linear function, thus the following simplifications are assumed: (i) integer discretization in (3) which restricts the capacity of cables, and may cause overestimation of electrical losses (this can be diminished by decimal round down, and by increasing discretization steps in (4) at the expense of augmenting the number of variables correspondingly). (ii) neglecting system states (cables failures) apart of the base state (no failures); however, this is the state with highest probability. (iii) power flow estimation in a conservative fashion, i.e., overestimating the incoming power flow by neglecting the total power losses downstream. All those simplifications may impact the final layout, however their conservative nature means rather over-designing than impacting the robustness.

2.3. Constraints

In case total electrical power losses are considered, the cable types set is $\boldsymbol{T'}$, otherwise $\boldsymbol{T}$; same logic for $\boldsymbol{U}/\boldsymbol{U'}$, t/t', and $u_t/u'_{t'}$. This applies for the forthcoming mathematical expressions.

The first stage constraints are presented first. These constraints are only defined by the first stage variables, i.e., the investment decision.

In case edge $[ij]$ is active in the solution, then one and only one cable type $t \in \boldsymbol{T}$ must be chosen, as expressed in the next equation

$$\sum_{t \in \boldsymbol{T}} x_{ij,t} = y_{ij} \quad \forall [ij] \in \boldsymbol{E} \tag{6}$$

A closed-loop (sunflower petals) collection system topology is forced through the following expression

$$\sum_{\substack{j \in \boldsymbol{N} \\ j \neq i}} y_{ij} = 2 \quad \forall l \in \boldsymbol{N}_{\mathrm{w}} : l = i \vee l = j \tag{7}$$

Limiting the number of feeders (upper limit of ϕ feeders) connected to the OSS is carried out by means of

$$\sum_{i \in \boldsymbol{N}_{\mathrm{w}}} y_{ij} \leq \phi \quad j = 1 \tag{8}$$

The set $\boldsymbol{\chi}$ stores pairs of edges $\{[ij], [uv]\}$, which are crossing each other. Excluding crossing edges in the solution is ensured by the simultaneous application of the next linear inequalities along with (6)

$$y_{ij} + y_{uv} \leq 1 \quad \forall \{[ij], [uv]\} \in \boldsymbol{\chi} \tag{9}$$

The no-crossing cables restriction is a practical requirement in order to avoid hot-spots, and potential single-points of failure caused by overlapping cables [9]. Constraint (9) exhaustively lists all combinations of crossings edges. The constraints in (6) ensure that no active edges are crossing or overlapping between each other. These constraints thus link the variables y_{ij} and $x_{ij,t}$.

The second stage constraints are now deployed. These constraints are only defined by the second stage variables, i.e., the operational aspects. They are defined by the flow conservation, which also avoids disconnected solutions, and is considered by means of one linear equality per wind turbine as per

$$\sum_{\substack{i \in \boldsymbol{N} \\ j \neq i}} \sum_{\omega \in \boldsymbol{\Omega}} \sum_{k \in \boldsymbol{K}} I_{ji}^{\omega,k} - I_{ij}^{\omega,k} + \delta_j^{\omega,k} = I_j^{\omega} \quad \forall j \in \boldsymbol{N}_{\mathrm{w}} \quad \forall \omega \in \boldsymbol{\Omega} \quad \forall k \in \boldsymbol{K} \tag{10}$$

The set of tender constraints, useful to link first and second stage constraints, are lastly presented.

The power flow distribution along the resultant electrical network is calculated using a DC power flow model (a linearized model of the AC power flow). Although DC power flow assumes no active power losses, nominal voltage at each bar, and no reactive power flow, it is typically used in unit commitment models due to its simplicity and computational efficiency [18]. The DC power flow is forced with the following equations

$$I_{ij}^{\omega,k} - \frac{1000 \cdot V_n \cdot (\theta_i^{\omega,k} - \theta_j^{\omega,k})}{\sqrt{3} \cdot X_t \cdot d_{ij}} - M \cdot (1 - x_{ij,t}) - M \cdot r_{ij}^k \leq 0 \quad \forall [ij] \in \boldsymbol{E} \quad t \in \boldsymbol{T} \quad \forall \omega \in \boldsymbol{\Omega} \quad \forall k \in \boldsymbol{K} \tag{11}$$

$$-I_{ij}^{\omega,k} + \frac{1000 \cdot V_n \cdot (\theta_i^{\omega,k} - \theta_j^{\omega,k})}{\sqrt{3} \cdot X_t \cdot d_{ij}} - M \cdot (1 - x_{ij,t}) - M \cdot r_{ij}^k \leq 0 \quad \forall [ij] \in \boldsymbol{E} \quad t \in \boldsymbol{T} \quad \forall \omega \in \boldsymbol{\Omega} \quad \forall k \in \boldsymbol{K} \tag{12}$$

where r_{ij}^k is a parameter equal to one if edge $[ij]$ is failed, and zero otherwise, X_t is the electrical reactance per meter of cable t (in case of inclusion of total electrical power losses, let $X_{t'} = h(t')$), and M is a big enough number to guarantee feasibility for those inactive or failed components.

The cable capacities are not exceeded by including the bilateral constraints:

$$\sum_{t \in \boldsymbol{T}} u_t \cdot x_{ij,t} \cdot (1 - r_{ij}^k) \geq I_{ij}^{\omega,k} \quad \forall [ij] \in \boldsymbol{E} \quad \forall \omega \in \boldsymbol{\Omega} \quad \forall k \in \boldsymbol{K} \tag{13}$$

$$\sum_{t \in \boldsymbol{T}} -u_t \cdot x_{ij,t} \cdot (1 - r_{ij}^k) \leq I_{ij}^{\omega,k} \quad \forall [ij] \in \boldsymbol{E} \quad \forall \omega \in \boldsymbol{\Omega} \quad \forall k \in \boldsymbol{K} \tag{14}$$

The current $I_{ij}^{\omega,k}$ may circulate either from i to j or viceversa.

Finally, Constraints (15) to (19) define the nature of the formulation by the variables definition, a MILP optimization program.

$$x_{ij,t} \in \{0, 1\} \quad \forall t \in \boldsymbol{T} \quad \forall [ij] \in \boldsymbol{E} \tag{15}$$

$$y_{ij} \in \{0, 1\} \quad \forall [ij] \in \boldsymbol{E} \tag{16}$$

$$-0.1 \leq \theta_i^{\omega,k} \leq 0.1 \quad \forall i \in \boldsymbol{N} \quad \forall \omega \in \boldsymbol{\Omega} \quad \forall k \in \boldsymbol{K} \tag{17}$$

$$-U \leq I_{ij}^{\omega,k} \leq U \quad \forall [ij] \in \boldsymbol{E} \quad \forall \omega \in \boldsymbol{\Omega} \quad \forall k \in \boldsymbol{K} \tag{18}$$

$$0 \leq \delta_i^{\omega,k} \leq I_i^{\omega,k} \quad \forall i \in \boldsymbol{N}_{\mathrm{w}} \quad \forall \omega \in \boldsymbol{\Omega} \quad \forall k \in \boldsymbol{K} \tag{19}$$

To summarize, the formulation of the MILP optimization program consists of the objective function (1) or (5), and the constraints defined in (6) - (19). Let this stochastic optimization program be denoted $P^{\boldsymbol{\Omega},\boldsymbol{K}}$.

3. Optimization framework

Since the two-stage variables scale-up exponentially as a function of the scenario tree size, the representative systems states must be limited [14]. The basic version of the stochastic optimization program presented in Section 2 encompasses the full set $\boldsymbol{E}$; each element $[ij]$ gives place to a system state k to form the system states set $\boldsymbol{K}$ (using the transformation function $\boldsymbol{K} = \Phi(\boldsymbol{E})$ which maps from edges set to system states set).

Nevertheless, the actual selected edges in a solution (i.e. a feasible point satisfying the optimality criteria) is only a subset $\boldsymbol{E'} \subset \boldsymbol{E}$; let the complement set $\boldsymbol{E''}$ contain the unused elements from $\boldsymbol{E}$, and let define the subset $\boldsymbol{E'''} \subset \boldsymbol{E''}$.

Trough an inactive edge $[ij]$ ($y_{ij} = 0$) there is no electrical current in any of the system scenarios according to (13) and (14). If there is no current through an edge, then its failure has no impact over the network power flow. This can be intuitively understood as comparing it with an open water tap which causes no spill when pipes are broken, as there is no flow of water. As a consequence, only the subset $\boldsymbol{K'} \subset \boldsymbol{K}$ (related to) is necessary and sufficient to obtain the optimum in $P^{\boldsymbol{\Omega},\boldsymbol{K}}$.

Let the necessary and sufficient set $\boldsymbol{K'}$ encompass:

$$\boldsymbol{K'} = k_\mathrm{o} \cup \boldsymbol{K_{E'}} \cup \boldsymbol{K_{E'''}} \tag{20}$$

Where $\boldsymbol{K_{E'''}}$ are the system states linked to the subset of unused edges $\boldsymbol{E'''}$, and $\boldsymbol{K_{E'}}$ to $\boldsymbol{E'}$.

The formal mathematical proof is not deployed in this article, but this particular characteristic reveals a contingency structure which can be exploited in order to simplify the full problem $P^{\boldsymbol{\Omega},\boldsymbol{K}}$. This contingency structure opens the door for a Progressive Contingency Incorporation (PCI) strategy, aiming at finding a proper set $\boldsymbol{K'}$ following an iterative approach. Algorithm 1 is presenting the PCI implementation.

A deterministic instance of the full problem is addressed in the first line. This means considering uniquely the scenario $\{\omega_\mathrm{n}, k_\mathrm{o}\}$. For this problem a valid assumption is to consider zero curtailed power. After this, the active edges of interest corresponding to the first stage optimization variables are stored as $\boldsymbol{E'}$, along with the obtained solution variables in $\boldsymbol{X}_\mathrm{ws}$ (where $\boldsymbol{X}_\mathrm{d}$ and $\boldsymbol{Y}_\mathrm{d}$ contains the solution sets corresponding to $x_{ij,t}$, and y_{ij} for the deterministic case, respectively). As no previous iteration has been conducted, cumulative solution variables are unavailable ($\boldsymbol{E'_\mathrm{o}}$). Since the second stage variables express contingency scenarios of the components delimited by the first stage variables, the tree Υ uniquely considers the failure states associated to those components. For the case presented in Algorithm 1, solely those feeders which satisfy the reliability level r_c, are subject to fail.

Acknowledging that not all cables have the same impact on energy curtailment in case of failure, parameter r_c defines the degree of connection towards the OSS. For example, $r_\mathrm{c} = 1$ considers only the main feeders (rooted at $i = 1$), defined as the cables leaving the OSS and connecting the WT at one end of the string. Accordingly, $r_\mathrm{c} = 2$ incorporates the main feeders, but expands to also include the cables connecting the next WTs in the string, and so on. With this definition of reliability level, the model can be further relaxed for large instances.

The Progressive Contingency Incorporation routine is started at line 4. The opening step is to intersect the current active edges set $\boldsymbol{E'}$, and the cumulative set $\boldsymbol{E'_\mathrm{o}}$. If the intersection set is equal to the current active edges $\boldsymbol{E'}$, then the process is terminated, otherwise more iterations are attempted. For the former case, the algorithm is stopped, with solution $[\boldsymbol{X}, \boldsymbol{Y}]$; for the latter case, the iterative process is continued to the subsequent iteration κ. Trivially, for $\kappa = 1$, $\boldsymbol{A} = \emptyset$. Therefore, in line 9 the union set is obtained to update $\boldsymbol{E'_\mathrm{o}}$. A new instance of the main problem is solved in line 10, using the initial point $\boldsymbol{X}_\mathrm{ws}$ (warm-start point), while considering the full wind power generation scenarios indicated by the user Ω, and the system states related to edges cumulatively installed in all iterations, ($\boldsymbol{K'} = \Phi(\boldsymbol{E'_\mathrm{o}})$).

When Algorithm 1 converges, the scenario criterion is met: the proper set $\boldsymbol{K'}$ is obtained; meaning that all representative systems states have been already considered.

1. $[\boldsymbol{X}_d, \boldsymbol{Y}_d] \leftarrow \arg P^{\boldsymbol{\Omega},\boldsymbol{K'}} : \Omega = \omega_n, \boldsymbol{K'} = k_o$
2. $\boldsymbol{E'} \leftarrow \boldsymbol{Y}_d = \{[ij]\} : y_{ij} = 1 \quad \forall [ij] \in \boldsymbol{E} : [ij]$ *satisfies reliability level* r_c
3. $\boldsymbol{E'_o} \leftarrow \emptyset, \boldsymbol{X}_{ws} \leftarrow \boldsymbol{X}_d \cup \boldsymbol{Y}_d$
4. **for** $(\kappa = 1 : 1 : \kappa_{max})$ **do**
5. $\quad \boldsymbol{A} \leftarrow \boldsymbol{E'} \cap \boldsymbol{E'_o}$
6. $\quad$ **if** $(\boldsymbol{E'} == \boldsymbol{A})$ **then**
7. $\qquad$ *Break*
8. $\quad$ **end if**
9. $\quad \boldsymbol{E'_o} \leftarrow \boldsymbol{E'} \cup \boldsymbol{E'_o}$
10. $\quad [\boldsymbol{X}, \boldsymbol{Y}] \leftarrow \arg P^{\boldsymbol{\Omega},\boldsymbol{K'}} : \Omega, \boldsymbol{K'} = \Phi(\boldsymbol{E'_o}) \cup k_o$ *with initial point* $\boldsymbol{X}_{ws}$. $\Upsilon = \{\Omega, \boldsymbol{K'}\}$
11. $\quad \boldsymbol{E'} \leftarrow \boldsymbol{Y} = \{[ij]\} : y_{ij} = 1 \quad \forall [ij] \in \boldsymbol{E} : [ij]$ *satisfies reliability level* r_c
12. $\quad \boldsymbol{X}_{ws} \leftarrow \boldsymbol{X} \cup \boldsymbol{Y}$
13. **end for**

Algorithm 1: Progressive Contingency Incorporation (PCI) Algorithm

4. Case study

The applicability of the method explained in Section 2.2.2 is illustrated using Ormonde OWF [19] as case study, due to its small size (30 WTs) and closed-loop structure. The experiments have been carried out on an Intel Core i7-6600U CPU running at 2.50 GHz and with 16 GB of RAM. The chosen solver is IBM ILOG CPLEX Optimization Studio V12.7.1 [20]. The main input parameters are shown in Table 1. A Mean Time To Repair (MTTR) per failure of 30 days (720 hours) is considered in this study [4]. The objective function (1) is applied in this case study as the main aim is to present the model's performance and quantitative comparison versus a deterministic version.

Table 1. Data inputs

P_n	V_n	Life	c_e	MTTR	$\boldsymbol{U}$	$\boldsymbol{C}$	n_w	υ	σ	ϕ	r_c
5 MW	33 kV	30 y	2.86 $\frac{€}{\mathrm{Ah}}$	720 h	$\{530, 655, 775\}$ A	$\{450, 510, 570\}$ k€/km	30	6	10	4	1

The power magnitudes are $\zeta^1 = 1$ (ω_n), $\zeta^2 = 0.5$, $\zeta^3 = 0.2$, and $\zeta^4 = 0$. The duration times account for the project lifetime (30 years) and considering 8760 hours per year: $\tau^1 = 65700$ hours (ω_n), $\tau^2 = 91980$ hours, $\tau^3 = 91980$ hours, and $\tau^4 = 13140$ hours. A cable failure probability is calculated as per $\psi^k = \frac{MTTR}{MTTR+MTBT\cdot\frac{8760}{d_{ij}}}$, with d_{ij} being the edge length where the component is installed. The results for this case study are obtained starting from a MTBF value of 178 years kilometres per failure, considered as the performance benchmark of medium voltage cables today [4], and decreasing it to an (extreme) value of 10, exploring the limits of the proposed model. Each MTBF value represents a different stochastic problem meaning that the model is run individually.

Quantitative assessment for the comparison between the output of the stochastic model ($[\boldsymbol{X}, \boldsymbol{Y}]$), and the output of the deterministic model ($[\boldsymbol{X}_\mathrm{d}, \boldsymbol{Y}_\mathrm{d}]$) is carried out. For the latter, a recourse problem is solved $Q([\boldsymbol{X}_\mathrm{d}, \boldsymbol{Y}_\mathrm{d}])$, defined as minimization of the expected costs (reliability costs) given the scenario tree (Υ) obtained from the wind power generation scenarios Ω, and the system states linked to $\boldsymbol{Y}_\mathrm{d}$.

For all the MTBF instances considered, an optimality gap of 0% has been set up, and a reliability level of $r_c = 1$ is assumed; this means that only those feeders connected directly to the OSS are subject to failure (the main feeders).

Due to the small size and the rather straightforward layout of the wind farm, the main difference between the deterministic and stochastic optimization, for the case of an (extreme) MTBF of 10, consists of the cable size of the main feeders (note colour code of cable sizes), as shown in Figure 2. For OWFs with more wind turbines and/or more irregular layout, the changes would likely expand to the connections between the wind turbines.

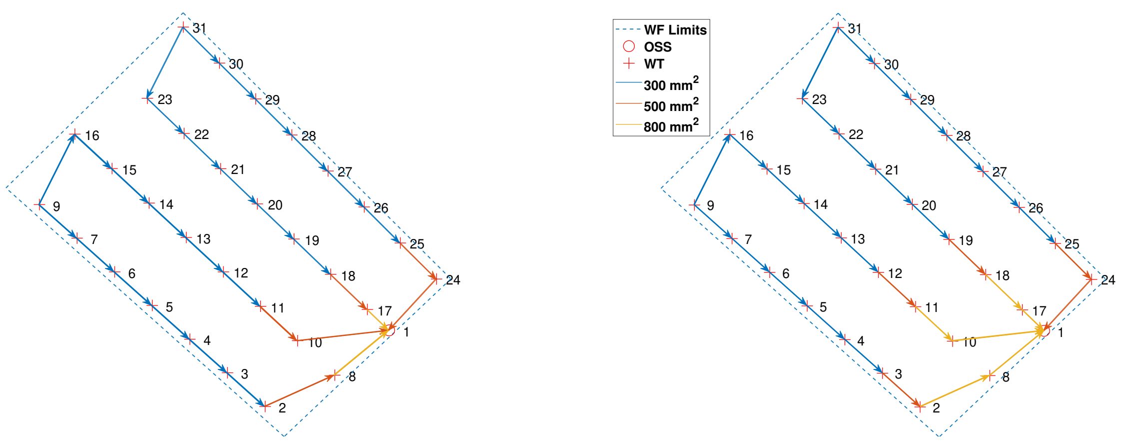

(a) Deterministic designed layout (b) Stochastic designed layout

Figure 2. Designed cables layouts for MTBF=10

The economic comparison between deterministic and probabilistic model (see Figure 3(a)), indicates that for MTBF values inferior to 30, the stochastic model provides a cheaper system in overall terms; this is achieved as reliability costs are lower at expense of more costly cable infrastructure (in this particular case only due to cable sizing). The values in Figure 3(a) are expressed as the percentage difference between the deterministic and stochastic model relative to the latter. The associated reliability costs for the deterministic designed layout are calculated through the aforementioned recourse problem; a DC power flow and undistpached energy are the main results for this particular task.

Conversely, beyond MTBF=30, the failures probabilities drop considerably, resulting in an equal weight for each cost unit (initial investment and reliability costs) in the objective function of the deterministic model. This basically means that the reliability costs become trivial, i.e. value of undispatched energy is low, and hence the focus is merely on the investment costs reduction. To compare the overall costs, the deterministic layout solution is run with the scenarios analyzed in the stochastic.

For large values of r_c, i.e. such that all edges are included in the reliability analysis, one could expect that the MTBF break-even point would move further to the right, that is, stochastic programming would provide overall more economic benefits even for less frequent failures rates, i.e. larger MTBF values.

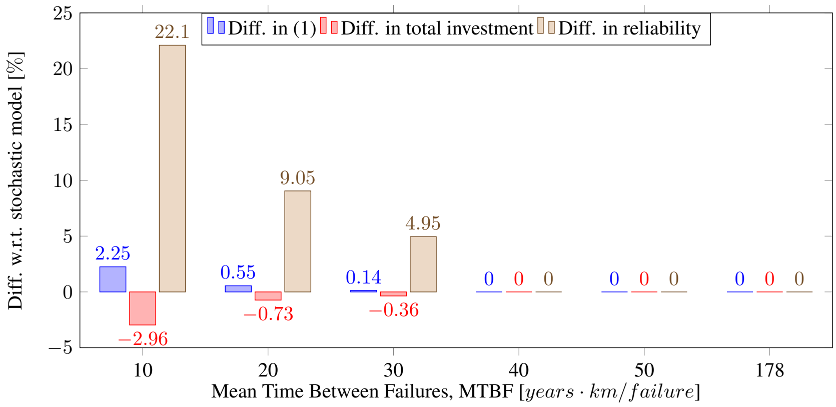

(a) Economic comparison. (Positive percentages mean savings using stochastic optimization)

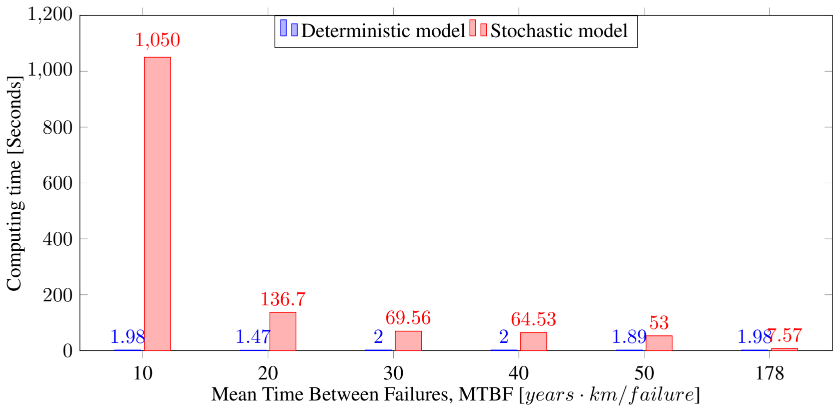

(b) Computing time comparison

Figure 3. Deterministic vs Stochastic Model for Closed-Loop Structure

Regarding computing times, shown in Figure 3(b), it is noticeable that the stochastic model's computational complexity is increasing for each MTBF value, as for instance, for a value of 10 the computing time is 530 times larger than the deterministic version. Likewise, the larger the MTBF, the more simplified the model becomes as the reliability costs share are decreasing. The deterministic cases on the other hand are independent to the failures rate and converge in couple of seconds (the small variations of computing time among the deterministic cases is merely due to CPU's performance).

5. Conclusions

A stochastic model to quantify the economic suitability of closed-loop collection system for OWFs is introduced in this manuscript. The objective function allows for simultaneous consideration of initial investment, total electrical power losses costs, and reliability costs. The focus of this work has been to describe the proposed model, presenting its main functionality through a rather simple case study.

Results of this article point out that in function of failure parameters, network topologies with redundant power paths may bring along significant cost benefits when applying stochastic optimization, compared to a simple deterministic approach. Choosing when to use a stochastic model is not trivial, as its complex mathematical structure has an considerable impact on the required computational resources. To somehow simplify this complexity, the contingency structure of the problem has been exploited analytically. Future work will focus on applying the method on several wind farm instances, both in terms of size (number of WTs) and layout (regular/irregular) for quantitatively comparing closed loop and radial network topologies.

References

[1] BVG Associates, Recognis and WindEurope 2019 Our Energy Our Future Tech. rep.
[2] Sun X, Huang D and Wu G 2012 *Energy* **41** 298–312 URL https://doi.org/10.1016/j.energy.2012.02.054
[3] ReNEWS 2017 Rampion suffers cable fault URL http://renews.biz/105889/rampion-suffers-cable-fault/.[Accessed Oct 29, 2018]
[4] Warnock J, McMillan D, Pilgrim J and Shenton S 2019 *Energies* **12** 1–12 URL https://doi.org/10.3390/en12142682
[5] CIGRE: Working Group B110 2009 Update of service experience of HV underground and submarine cables Tech. rep. URL https://e-cigre.org/publication/ELT_243_3-update-of-service-experience-of-hv-underground-and-submarine-cable-systems.[Accessed March 30, 2020]
[6] CIGRE: Working Group B121 2009 Third-Party Damage to Underground and Submarine Cables Tech. rep. URL https://e-cigre.org/publication/398-third-party-damage-to-underground-and-submarine-cables.[Accessed March 30, 2020]
[7] Pérez-Rúa J A and Cutululis N A 2019 *IEEE Access* **7** 85796–85811 URL https://doi.org/10.1109/ACCESS.2019.2925873
[8] Fischetti M and Pisinger D 2018 *European Journal of Operational Research* **270** 917–930 URL https://doi.org/10.1016/j.ejor.2017.07.061
[9] Bauer J and Lysgaard J 2015 *Journal of the Operational Research Society* **66** 360–368 URL https://doi.org/10.1057/jors.2013.188
[10] Pillai A C, Chick J, Johanning L, Khorasanchi M and De Laleu V 2015 *Engineering Optimization* **47** 1689–1708 URL https://doi.org/10.1080/0305215X.2014.992892
[11] Klein A and Haugland D 2017 *Annals of Operations Research* **272** 373–388 URL https://doi.org/10.1007/s10479-017-2581-5
[12] Pérez-Rúa J A, Stolpe M, Das K and Cutululis N A 2020 *IEEE Transactions on Power Systems* **35** 2256–2267
[13] Banzo M and Ramos A 2011 *IEEE Transactions on Power Systems* **26** 1338–1348 URL https://doi.org/10.1109/TPWRS.2010.2075944
[14] Lumbreras S, Ramos A and Cerisola S 2013 *IEEE Transactions on Power Systems* **28** 1452–1460 URL https://doi.org/10.1109/TPWRS.2012.2225077
[15] Lumbreras S and Ramos A 2013 *IEEE Transactions on Power Systems* **28** 1434–1441 URL https://doi.org/10.1109/TPWRS.2012.2204906
[16] Calixto E 2016 *Gas and Oil Reliability Engineering* 2nd ed (Gulf Professional Publishing) URL https://www.sciencedirect.com/book/9780128054277/gas-and-oil-reliability-engineering#book-info[Accessed March 05, 2020]
[17] Billinton R and Allan R N 1992 *Reliability Evaluation of Engineering Systems: Concepts and Techniques*
[18] Grainger J J and Stevenson W D J 1994 *Power System Analysis* 2nd ed (McGraw-Hill Education)
[19] Vatenfall Ormonde Offshore Wind Farm URL https://powerplants.vattenfall.com/ormonde.[Accessed Feb 5, 2020]
[20] IBM 2015 IBM ILOG CPLEX Optimization Studio CPLEX User Manual Tech. rep. URL https://www.ibm.com/support/knowledgecenter.[Accessed April 11, 2019]